IEIE Transactions on Smart Processing and Computing, vol. 4, no. 4, August 2015
http://dx.doi.org/10.5573/IEIESPC.2015.4.4.251

Pair-Wise Serial ROIC for Uncooled Microbolometer Array

Syed Irtaza Haider[1], Sohaib Majzoub[2], Mohammed Alturaigi[1] and Mohamed Abdel-Rahman[1]

[1]College of Engineering, King Saud University, Riyadh, KSA {sirtaza, mturaigi, mabdelrahman}@ksu.edu.sa
[2]Electrical and Computer Engineering, University of Sharjah, UAE sohaib.majzoub@ieee.org

***** Corresponding Author: Syed Irtaza Haider

Received June 20, 2015; Revised July 15, 2015; Accepted August 24, 2015; Published August 31, 2015

** Short Paper*

** Extended from a Conference: Preliminary results of this paper were presented at the ICEIC 2015. This present paper has been accepted by the editorial board through the regular reviewing process that confirms the original contribution.*

***Abstract*:** This work presents modelling and simulation of a readout integrated circuit (ROIC) design considering pair-wise serial configuration along with thermal modeling of an uncooled microbolometer array. A fully differential approach is used at the input stage in order to reduce fixed pattern noise due to the process variation and self-heating–related issues. Each pair of microbolometers is pulse-biased such that they both fall under the same self-heating point along the self-heating trend line. A ±10% process variation is considered. The proposed design is simulated with a reference input image consisting of an array of 127x92 pixels. This configuration uses only one unity gain differential amplifier along with a single 14-bit analog-to-digital converter in order to minimize the dynamic range requirement of the ROIC

***Keywords*:** Microbolometer, Process variation, ROIC, Self-heating thermal imaging system

1. Introduction

Infrared uncooled thermal imagers have been employed in a wide range of civilian and military applications for smartphone cameras, industrial process monitoring, driver night vision enhancement, and military surveillance [1-3]. Micro-electro-mechanical system (MEMS) microbolometer thermal detectors are the most widely used pixel element detectors in today's infrared uncooled thermal imaging cameras.

Microbolometer sensor arrays are fabricated using MEMS technology, but they suffer from process variation, which introduces fixed pattern noise (FPN) in detector arrays [4]. At the early stage of sensor fabrication, a sensor's resistance discrepancy of ±10% is expected [5]. A microbolometer detector changes its resistance when exposed to IR radiation due to its thermally sensitive layer. If the target temperature differs from the ambient temperature, i.e. ΔTscene, by 1K, it results in a temperature increase in the microbolometer membrane on the order of 4mK [2].

These thermal detectors need to be electrically biased during the readout in order to monitor the change in resistance. Electrical biasing generates heat, which results in self-heating of the microbolometer detector and causes a change in resistance. Heat generated by self-heating cannot be quickly dissipated through thermal conduction to the substrate. It results in a change in temperature due to self-heating much higher than a change in temperature due to incident radiation [6, 7].

FPN and self-heating results in major degradation and poor performance of the thermal imaging system, and hence, imposes a strict requirement on ROIC for noise compensation in order to detect the actual change due to infrared radiation.

Readout topologies extensively discussed in the literature are pixel-wise [8], column-wise [5] and serial readout [9]. Pixel-wise readout improves noise performance of the microbolometer by increasing the integration time up to the frame rate [10]. Column-wise readout reduces the number of amplifiers and integrators, which thus serves as a good compromise between the silicon area and parallel components [10, 11]. Serial readout architecture is read pixel by pixel, and therefore, it requires only one amplifier and integrator, resulting in low power consumption and a compact layout [10].

This paper focuses on ROIC design considering the impact of process variation and self-heating on performance. Pair-wise, time-multiplexed, column-wise configuration is used, in which one pair of microbolometers is selected at a

time. Readout is performed differentially during the pulse duration. The focal plane array (FPA) consists of 127x92 normal microbolometers and one row of blind microbolometers to provide a reference for the ROIC. This paper is organized as follows. Section 2 describes the literature review. Section 3 covers thermal modelling of an uncooled microbolometer. Section 4 explains the pair-wise serial readout architecture in detail, along with an ROIC simulator. Finally, we conclude this paper in the last section.

2. Literature Review

This section summarizes the studies conducted on different aspects of thermal imaging systems. Some of the important figures of merit are discussed, which are helpful in evaluating the performance of infrared detectors. Some of the commonly used thermal sensing materials that influence the sensitivity of microbolometers are discussed. The focal plane array and the readout integrated circuit are two major building blocks of a thermal imaging system.

The operation of a thermal imaging system starts with the absorption of the incident infrared radiation by the uncooled microbolometer detector array. Each microbolometer detector changes its resistance based on the absorbed infrared radiation. It is important to establish criteria with which different infrared thermal detectors are compared. The most important figures of merit are the thermal time constant (τ), noise equivalent power (NEP), responsivity (□), noise equivalent temperature difference (NETD) and detectivity (D*) [2, 10, 12-14]. The performance of a microbolometer is influenced by the thermal sensing material. There are three types of material that are suitable for the bolometer: metal, semiconductor and superconductor. Metal and semiconductor microbolometers operate at room temperature, whereas superconductor microbolometers require cryogenic coolers. Typical materials used for microbolometers are titanium, vanadium oxide and amorphous silicon.

Single input mode and differential input mode ROIC designs are widely used at the reading stage of the ROIC in order to detect the resistance value of a microbolometer and to generate the voltage value. Differential input mode assumes that the adjacent pixels are subjected to a small radiation difference, and hence, results in a small resistance change, causing a similar voltage change for adjacent microbolometer cell resistances that can be read and handled by a differential amplifier [15].

In addition, process variation creates resistance discrepancy among the sensors during the wafer process. A differential input mode ROIC design attempts to cancel these resistance differences among microbolometers using the differentiation method. Thus, it suppresses the common error and amplifies the differential signal. The conventional single input mode, on the other hand, is known to be inefficient at compensating for fixed pattern noise since it has low immunity to process variation. A comparison between single input mode ROIC and differential input mode ROIC to decrease the error due to process variation was presented [16].

Pixel-parallel, serial and column-wise readout architectures have mostly been discussed in the past. Parallel readout increases power consumption and the complexity of the readout, whereas serial readout reduces the speed of a thermal imager due to its time-multiplexed nature. Pixel-parallel readout, also known as frame-simultaneous readout, is used for very-high-speed thermal imaging systems. Each pixel in a cell array consists of detector, amplifier and integrator. The pixel-wise readout architecture is suitable for very-low-noise applications because it reduces Johnson noise, one of the largest noise sources. The disadvantage of the pixel-parallel architecture is the complex readout resulting in a large pixel area and extensive power dissipation. Conventional ROIC uses column-wise readout because this architecture serves as a good compromise between the speed and complexity of readout due to parallel components. Finally, the last readout architecture is serial readout. This approach uses only one amplifier and one analog-to-digital converter (ADC) to perform the readout due to the time-multiplexed nature of its readout. Advantages with serial readout are compact layout and low power consumption.

3. Thermal Modeling of a Microbolometer

Self-heating is an unavoidable phenomenon which causes the temperature of a thermal detector to rise, even though the bias duration is much smaller, compared to the thermal time constant of the detector. The heat balance equation of a microbolometer, including self-heating, can be written as:

$$H\frac{d\Delta T}{dt}+G\Delta T=P_{BIAS}+P_{IR} \tag{1}$$

where H is the thermal capacitance, G is the thermal conductance of the microbolometer, P_{BIAS} is the bias power, and P_{IR} is the infrared power absorbed by the microbolometer detector. For metallic microbolometer materials, resistance R_B has linear dependence on temperature, and can be expressed as:

$$R_B\left(t_{BIAS}\right)=R_0\left(1+\alpha\Delta T\left(t_{BIAS}\right)\right) \tag{2}$$

where α is the temperature coefficient of resistance (TCR) of the detector, R_0 is the nominal resistance, and $\Delta T(t_{BIAS})$ is the temperature change due to self-heating during pulse biasing, and is given by:

$$\Delta T\left(t_{BIAS}\right)=T-T_0=\frac{P_{BIAS}\left(t_{BIAS}\right)\times t_{BIAS}}{G.\tau} \tag{3}$$

where τ is the thermal time constant. Under normal conditions, $t_{BIAS} << \tau$ and ΔT due to self-heating is independent of thermal conductance. If I_{BIAS} is the constant bias current applied to the microbolometer during the readout, self-heating power can be expressed as:

$$P_{BIAS}\left(t_{BIAS}\right)=I_{BIAS}^2R_B\left(t_{BIAS}\right) \tag{4}$$

By solving the above equation using (2) and (3),

$$P_{BIAS}\left(t_{BIAS}\right)=\frac{I_{BIAS}^2 R_0 H}{H-I_{BIAS}^2 t_{BIAS} R_0 \alpha} \quad (5)$$

When FPA is exposed to incident radiation, the difference in radiant flux incoming to the microbolometer can be estimated as

$$\Delta\phi_{IR}=\frac{A_b \Delta T_{scene}}{4F^2}\left(\frac{dP}{dT}\right)_{300K,\Delta\lambda} \quad (6)$$

where ΔT_{scene} is the difference in temperature between target and ambient temperatures, and $(dP/dT)_{300K,\Delta\lambda}$ is the change in power per unit area with respect to temperature change radiated by a black body at an ambient temperature in the wavelength interval 8μm-14μm. The temperature change due to the absorbed infrared power is given by

$$\Delta T_{IR}=\frac{\Delta\phi_{IR}}{G} \quad (7)$$

Resistance change of a microbolometer detector due to change in scene temperature can be evaluated as

$$\Delta R_{IR}=R_0\left(\alpha.\beta.\phi_{\Delta\lambda}.\varepsilon_{\Delta\lambda}.\Delta R_{IR}\right) \quad (8)$$

where β is the fill factor of the microbolometer, $\Phi_{\Delta\lambda}$ is the transmission of optics, and $\varepsilon_{\Delta\lambda}$ is the absorption of microbolometer membrane in an infrared region. When both incident and bias power are zero, the temperature of the microbolometer cools down based on the equation below:

$$T_{COOL}(t)=T_B\, e^{\left(\frac{-t}{\tau}\right)} \quad (9)$$

where T_B is the temperature of the microbolometer at the end of pulse biasing. Infrared system parameters mentioned in Table 1 are taken from [5].

4. Thermal Modeling of a Microbolometer

Fig. 1 demonstrates the flowchart of the ROIC simulator. Temperature mapping of a thermal image is performed at the beginning. For each pixel, ΔT_{scene} is calculated based on the target temperature and ambient temperature. An infrared radiation model evaluates the difference in incoming flux $\Delta\Phi_{IR}$, the change in bolometer temperature ΔT_{IR}, and the resistance change in the bolometer due to the absorbed incident power ΔR_{IR}.

$$R_{TOTAL}=R_0+R_{PV}+R_{IR} \quad (10)$$

where R_{PV} is resistance due to process variation and is a ±10% deviation from nominal resistance, and R_{IR} is the change in microbolometer resistance due to incident radiation. Parameters mentioned in Table 1 and synchronization pulse sequence, as mentioned in Table 2, are provided to the ROIC simulator. It evaluates self-heating power, temperature drift and change in resistance due to pulse biasing.

A 14-bit ADC is used to convert the signal to digital representation. The blind microbolometer exhibits the same thermal characteristics as that of a normal micro-

Table 1.Thermal Parameters of the Microbolometer.

Parameters	Values
Nominal Resistance, R_0 (kΩ)	100
Pulse Duration, t_{BIAS} (μs)	6
Bias Current, I_{BIAS} (μA)	20
Ambient Temperature, T_0 (K)	300
Thermal Time Constant, τ (ms)	11.7
Temperature Coefficient of Resistance, α (%/K)	-2.6
Thermal Conductance, G (W/K)	3.7e-8
Thermal Capacitance, H (J/K)	4.34e-10
Optics F/Number	1
Area of Microbolometer Pixel, A_b(m^2)	6.25e-10
Fill Factor of Microbolometer, β (%)	62
Transmission of Infrared Optics, $\Phi_{\Delta\lambda}$ (%)	98
Absorption of microbolometer membrane, $\varepsilon_{\Delta\lambda}$ (%)	92
Temperature Contrast $(dP/dT)_{300K,\Delta\lambda}$ ($WK^{-1}m^{-2}$)	2.624
FPA Size	128 × 92
Frame Rate (frames per second)	10

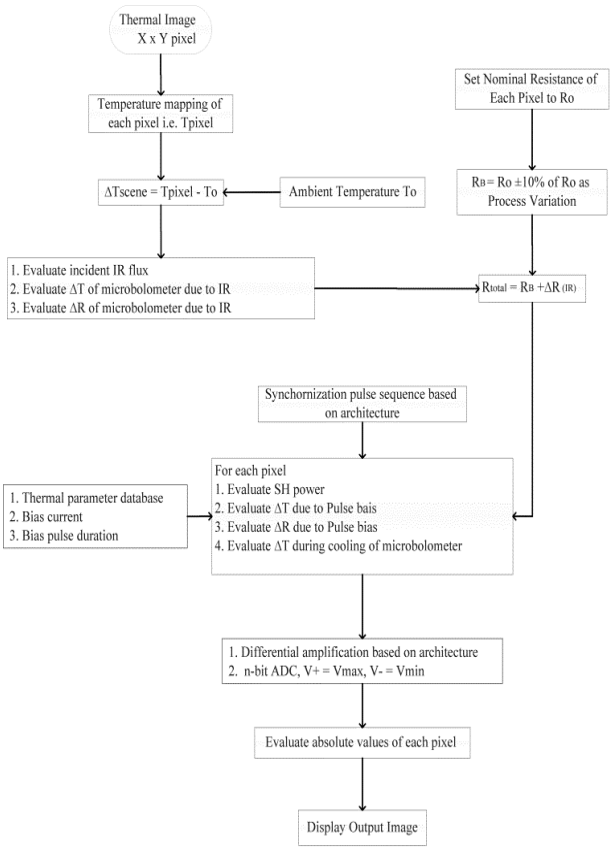

Fig. 1. ROIC Simulator Flowchart.

Table 2. Pulse sequence for pair-wise serial ROIC architecture, where BD is microbolometer detector.

Pulse	Selected Microbolometer Detector (BD) Pair	
1	Blind (1,i) and BD(2,i)	i = 1,2,3,…Y,
2	BD (3,i) and BD(4,i)	
:	:	
(X/2)	BD (X-1,i) and BD (X, i)	
(X/2) + 1	BD (2,i)and BD (3,i)	
:	:	
(X-1)	BD (X-2,i) and BD (X-1,i)	

bolometer but remains unaffected by incident radiation, and thus, serves as a reference point. Each microbolometer, either blind or normal, is connected with a current source through a p-channel metal-oxide-semiconductor (PMOS) switch. The gate of the PMOS switch is controlled through the digital circuitry that generates the pulse sequence based on the serial readout topology. Absolute values of each pixel are then calculated based on the reference blind microbolometer after all values are converted to the digital domain.

Fixed pattern noise correction is achieved by performing the complete readout under the dark condition. This measurement takes place when the focal plane array is not exposed to any incident power, and it is considered the reference value for each pixel. Later, every pixel reading has to be adjusted based on the pixel's reference point taken during the dark condition.

5. Pair-wise Serial Readout Architecture

Pair-wise serial readout architecture selects and bias one pair of microbolometers at a time, and the readout is performed differentially. A pair of microbolometers is biased twice during a frame rate, and the reading is performed differentially. Once the readout of the selected pair is finished, bias current source is switched to the next pair of microbolometers. The recently biased detector pair is left to cool off until the next pulse (for the next reading within the same frame rate) is applied. A blind microbolometer is biased once in a column with the first normal microbolometer, and it exhibits the same temperature drift due to self-heating as normal microbolometers, which can also be drastically minimized using a differential approach. The normal microbolometers are read twice with each adjacent neighbor, except for the last normal microbolometer. Table 2 shows the pulse sequence based on pair-wise serial configuration, where X is the number of rows and Y is the number of columns.

Consider a case for serial readout architecture where,

$T_{WAIT} = 2\mu s$, $T_{BIAS} = 6\mu s$,
$T_{COLUMN} = (T_{WAIT} + T_{BIAS}) * (X - 1)$
$T_{COLUMN} = (2\mu s + 6\mu s) * (128 - 1) = 10.16ms$
$T_{FRAME} = T_{COLUMN} * Y$
$T_{FRAME} = 10.16ms * 92 = 93.472ms$

The serial architecture is time-multiplexed; thus, only one pair of microbolometers is read during a single pulse duration. Thus, the minimum time to perform the readout of a single frame of a 127x92 pixel focal plane array is approximately 100ms for a T_{BIAS} of 6µs, and approximately 150ms for a T_{BIAS} of 10µs. This constraint limits the thermal imager to a maximum frame rate of 10 frames per second and 6 frames per second, respectively.

The following are the calculations of the start time of the pulse for the microbolometer in the tenth column second row, i.e. microbolometer (2, 10):

$T_{WAIT} = 2\mu s$, $T_{BIAS} = 6\mu s$,
$T_{COLUMN} = (T_{WAIT} + T_{BIAS}) * (X - 1)$

where X is the number of rows. It means, in order to perform the readout of a complete column, X-1 pulses are required. For the first pulse for microbolometer (2, 10):

$T_{PULSE1\ START} = T_{COLUMN} * 9 + T_{WAIT}$
$T_{PULSE1\ START} = 9.146ms$
$T_{PULSE1\ END} = T_{PULSE1\ START} + T_{BIAS}$
$T_{PULSE1\ END} = 9.146ms + 6\mu s = 9.152ms$

Similarly, the time of the second pulse for microbolometer (2, 10) is calculated as follows:

$T_{PULSE2\ START} = T_{PULSE1\ END} + ((X/2) - 1)T_{BIAS} + (X/2)T_{WAIT}$
$T_{PULSE2\ START} = 9.152ms + 63*T_{BIAS} + 64*T_{WAIT}$
$T_{PULSE2\ START} = 9.658ms$
$T_{PULSE2\ END} = T_{PULSE2\ START} + T_{BIAS}$
$T_{PULSE2\ END} = 9.658ms + 6\mu s = 9.664ms$

Before the second pulse for the same microbolometer arrives, the cooling time of a microbolometer is evaluated as follows:

$T_{COOL1} = T_{PULSE2\ START} - T_{PULSE1\ END}$
$T_{COOL1} = 9.658ms - 9.152ms = 506\mu s$

After the second pulse, cooling time of the microbolometer is evaluated as

$T_{COOL2} = T_{FRAME} - T_{PULSE2\ END}$
$T_{COOL2} = 100ms - 9.658ms = 90.142ms$

6. Simulation Results

Self-heating of a microbolometer causes the resistance of the microbolometer to drop due to its negative TCR. The resistance drop due to self-heating is of higher magnitude than the resistance drop due to incident infrared radiation, and thus imposes a strict requirement on the dynamic range of the ROIC. In order to relax this requirement, the microbolometers are pulse biased during the readout time, and the voltage drop due to self-heating is minimized.

Electrical biasing generates Joule heating and causes a change in the resistance of the microbolometer detector.

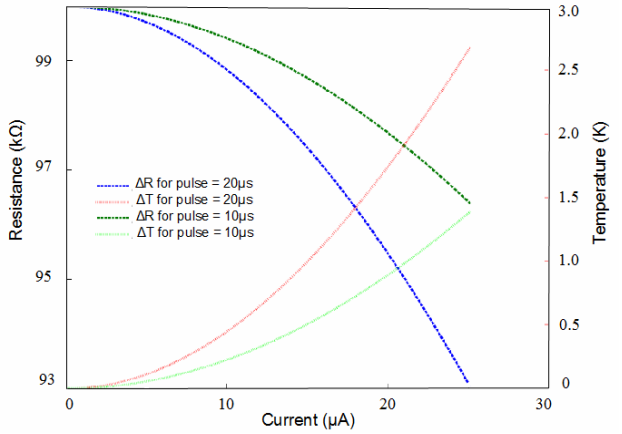

Fig. 2. Microbolometer self-heating for t_{BIAS}= 20μs and t_{BIAS}=10μs.

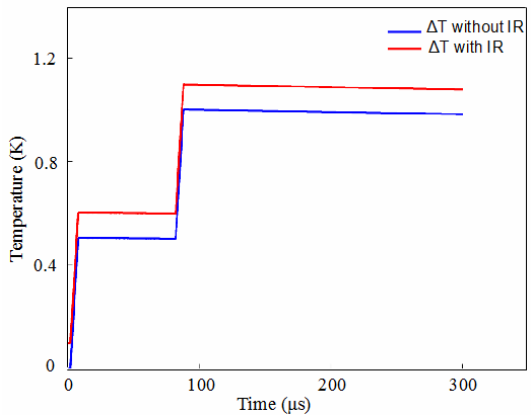

Fig. 3. Variation in microbolometer temperature with and without IR.

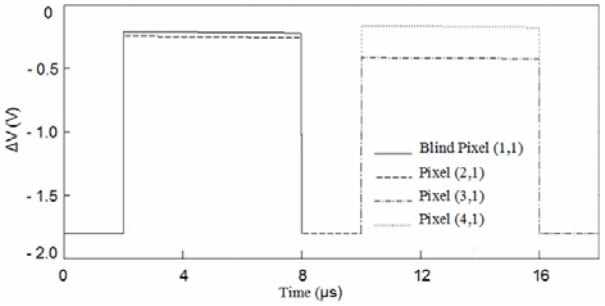

Fig. 4. Voltage variation of pixel (1,1) and pixel (2,1), and differential readout.

(a) (b)

Fig. 5. (a) Input thermal image 127 × 92, and (b) ROIC output.

Even though the bias duration is much shorter than the thermal time constant of the microbolometer detector, it still results in a significant rise in the temperature of the detector. This is due to the fact that applied bias power is much higher, compared to infrared absorbed power. It results in a much higher change in temperature due to self-heating, compared to incident radiation. Heat generated by self-heating cannot be quickly dissipated through thermal conduction to the substrate. Readout circuits are required to have complex circuit design and a high dynamic range, if self-heating not compensated for. Thus, self-heating must be compensated for in order to improve the performance of readout circuit, and eventually, the thermal imaging system.

In this work, microbolometers are pulse biased with a nominal value of bias current. If the bias current is too high, or biased for a long duration, it will result in excessive heating and permanent damage to the thermal detectors. Similarly, if the bias current is too low, it will result in low responsivity in the microbolometers. If the microbolometers are biased for a long duration, it will result in high temperature drift in the microbolometers due to self-heating.

Fig. 2 demonstrates the effect of self-heating by measuring resistance versus bias current for a pulse duration of 20μs and 10μs. For a pulse duration of 20μs, increasing the bias current from 1μA to 25μA results in a decrease in the nominal resistance of the microbolometer by approximately 7000Ω, which is equivalent to a temperature rise of 2.5K. In order to minimize the impact of self-heating, one way is to reduce the bias current to the lowest practical value, as shown in Fig. 2.

The thermal time constant of the microbolometer, along with time-multiplexed integration, limits the maximum frame rate of the thermal imaging system. For an FPA of 128x92 pixels, and by using the proposed pulse sequence, each pair of microbolometers can be selected for a pulse duration of 6μs with 10 frames per second. Fig. 3 shows the temperature variation of microbolometer pixel (2, 1) due to self-heating when given two pulses, one at t = 2μs and the second at t = 82μs. From t = 8μs to t = 82μs and from t = 88μs to t = tframe, both incident and bias power are zero, and hence, the bolometer cools down, as per (9), where tframe is the total time for the readout.

Fig 4 shows the voltage variation of reference microbolometer (1, 1) and normal microbolometers (2, 1), (3, 1) and (4, 1) during the readout. Few things can be concluded from the figure. Only one pair of micro-bolometers is biased at a time, and the voltage variation during the readout period is different for each micro-bolometer, even when there is no input power. This is due to the fact that during fabrication, microbolometers suffer from process variation due to process immaturity. Individual

slopes of reference for microbolometer (1, 1) and normal microbolometer (2, 1) are 5.348mV/µs and 4.2mV/µs, respectively. Both the microbolometers have different slopes, because they have different nominal resistances before the readout.

Fig. 5(a) shows the input thermal image to an ROIC simulator [17], which is 320 × 240 but cropped to 127 × 92 for simulation purposes. Fig. 5(b) shows the output image of the simulator using the proposed architecture, mapping a temperature change of about 12°C. Fixed pattern noise can be seen in the output image.

7. Conclusion

The ROIC model presented in this paper uses a pulse bias current scheme to reduce the effect of self-heating. Simulation results show that the temperature drift due to self-heating is compensated for by using differential readout, but it is not completely eliminated due to the consideration of a very high resistance discrepancy of ±10% due to process variation. A pulse sequence to each pair of microbolometers is provided, such that they both fall under the same self-heating point along the self-heating trend line, i.e. the pair picked is such that both are biased the same number of times. The proposed architecture for the ROIC requires one differential amplifier and one 14-bit ADC in order to reduce the dynamic range requirement, power dissipation and area at the expense of a longer readout time for a large focal plane array.

Acknowledgement

This work was supported by the NSTIP strategic technologies program number 12-ELE2936-02 in the Kingdom of Saudi Arabia.

References

[1] M. Perenzoni, D. Mosconi, and D. Stoppa, "A 160× 120-pixel uncooled IR-FPA readout integrated circuit with on-chip non-uniformity compensation," in *ESSCIRC, 2010 Proceedings of the*, 2010, pp. 122-125. Article (CrossRef Link)

[2] B. F. Andresen, B. Mesgarzadeh, M. R. Sadeghifar, P. Fredriksson, C. Jansson, F. Niklaus, A. Alvandpour, G. F. Fulop, and P. R. Norton, "A low-noise readout circuit in 0.35-µm CMOS for low-cost uncooled FPA infrared network camera," *Infrared Technology and Applications XXXV,* vol. 7298, pp. 72982F-72982F-8, 2009. Article (CrossRef Link)

[3] P. Neuzil and T. Mei, "A Method of Suppressing Self-Heating Signal of Bolometers," *IEEE Sensors Journal,* vol. 4, pp. 207-210, 2004. Article (CrossRef Link)

[4] S. J. Hwang, H. H. Shin, and M. Y. Sung, "High performance read-out IC design for IR image sensor applications," *Analog Integrated Circuits and Signal Processing,* vol. 64, pp. 147-152, 2009. Article (CrossRef Link)

[5] D. Svärd, C. Jansson, and A. Alvandpour, "A readout IC for an uncooled microbolometer infrared FPA with on-chip self-heating compensation in 0.35 µm CMOS," *Analog Integrated Circuits and Signal Processing,* vol. 77, pp. 29-44, 2013. Article (CrossRef Link)

[6] X.Gu, G.Karunasiri, J.Yu, G.Chen, U.Sridhar, and W.J.Zeng, "On-chip compensation of self-heating effects in microbolometer infrared detecto arrays," *Sensors and Actuators A: Physical,* vol. 69, pp. 92-96, 1998. Article (CrossRef Link)

[7] P. J. Thomas, A. Savchenko, P. M. Sinclair, P. Goldman, R. I. Hornsey, C. S. Hong, and T. D. Pope, "Offset and gain compensation in an integrated bolometer array," 1999, pp. 826-836. Article (CrossRef Link)

[8] C. H. Hwang, C. B. Kim, Y. S. Lee, and H. C. Lee, "Pixelwise readout circuit with current mirroring injection for microbolometer FPAs," *Electronics Letters,* vol. 44, pp. 732-733, 2008. Article (CrossRef Link)

[9] S. I. Haider, S. Majzoub, M. Alturaigi, and M. Abdel-Rahman, "Modeling and Simulation of a Pair-Wise Serial ROIC for Uncooled Microbolometer Array," in *ICEIC 2015*, Singapore, 2015.

[10] D. Jakonis, C. Svensson, and C. Jansson, "Readout architectures for uncooled IR detector arrays," *Sensors and Actuators A: Physical,* vol. 84, pp. 220-229, 2000. Article (CrossRef Link)

[11] S. I. Haider, S. Majzoub, M. Alturaigi, and M. Abdel-Rahman, "Column-Wise ROIC Design for Uncooled Microbolometer Array," presented at the International Conference on Information and Communication Technology Research (ICTRC), Abu-Dhabi, 2015. Article (CrossRef Link)

[12] R. K. Bhan, R. S. Saxena, C. R. Jalwania, and S. K. Lomash, "Uncooled Infrared Microbolometer Arrays and their Characterisation Techniques," *Defence Science Journal,* vol. Vol. 59, pp. 580-589, 2009.

[13] R. T. R. Kumar, B. Karunagaran, D. Mangalaraj, S. K. Narayandass, P. Manoravi, M. Joseph, V. Gopal, R. K. Madaria, and J. P. Singh, "Determination of Thermal Parameters of Vanadium oxide Uncooled Microbolometer Infrared Detector," *International Journal of Infrared and Millimeter Waves,* vol. 24, pp. 327-334, 2003. Article (CrossRef Link)

[14] J.-C. Chiao, F. Niklaus, C. Vieider, H. Jakobsen, X. Chen, Z. Zhou, and X. Li, "MEMS-based uncooled infrared bolometer arrays: a review," *MEMS/MOEMS Technologies and Applications III,* vol. 6836, pp. 68360D-68360D-15, 2007. Article (CrossRef Link)

[15] S. J. Hwang, A. Shin, H. H. Shin, and M. Y. Sung, "A CMOS Readout IC Design for Uncooled Infrared Bolometer Image Sensor Application," presented at the IEEE ISIE, 2006. Article (CrossRef Link)

[16] S. J. Hwang, H. H. Shin, and M. Y. Sung, "A New CMOS Read-out IC for Uncooled Microbolometer Infrared Image Sensor," International Journal of Infrared and Millimeter Waves, vol. 29, pp. 953-965, 2008. Article (CrossRef Link)

[17] *SPI infrared*. Available: Article (CrossRef Link)

Syed Irtaza Haider received his BE degree in Electronics Engineering from National University of Sciences and Technology (NUST), Pakistan, in 2010 and MS degree in Electronics Engineering from King Saud University (KSU), Saudi Arabia, in 2015. Currently, he is a researcher at Embedded Computing and Signal Processing Lab (ECASP) at the King Saud University. His research interest includes signal processing, mixed signal design and image processing. He is a student member IEEE.

Sohaib Majzoub completed his BE in Electrical Engineering, Computer Section at Beirut Arab University 2000, Beirut Lebanon, and his ME degree from American University of Beirut, 2003 Beirut Lebanon. Then he worked for one year at the Processor Architecture Lab at the Swiss Federal Institute of Technology, Lausanne Switzerland. In 2010, he finished his PhD working at the System-on-Chip research Lab, University of British Columbia, Canada. He worked for two years as assistant professor at American University in Dubai, Dubai, UAE. He then worked for three years starting in 2012 at King Saud University, Riyadh, KSA, as a faculty in the electrical engineering department. In September 2015, he joined the Electrical and Computer Department at the University of Sharjah, UAE. His research field is delay and power modeling, analysis, and design at the system level. He is an IEEE member.

Dr. Muhammad Turaigi is a professor of Electronics at the EE department, College of Engineering King Saud University. He got his PhD from the department of Electrical Engineering Syracuse University, Syracuse NY, USA in the year 1983. His PhD thesis is in the topic of parallel processing. In 1980 he got his MSc from the same school. His B.Sc. is from King Saud University (formerly Riyadh University) Riyadh Saudi Arabia. In Nov. 1983 He joined the department of Electrical Engineering, King Saud University. He teaches the courses in digital and analog electronic circuits. He has more than 40 published papers in refereed journals and international conferences. His research interest is in the field of parallel processing, parallel computations, and electronic circuits and instrumentation. He was the director of the University Computer Center from July/1987 until Nov/1991. He was a member of the University Scientific Council from July/1999 until June/2003.

Dr. Mohamed Ramy is an Assistant Professor in the Electrical Engineering Department, King Saud University, Riyadh, Saudi Arabia. He was previously associated with Prince Sultan Advanced Technologies Research Institute (PSATRI) as the Director of the Electro-Optics Laboratory (EOL). He has a PhD degree in Electrical Engineering from UCF (University of Central Florida), Orlando, USA. He has over 10 years of research and development experience in infrared/millimeter wave detectors and focal plane arrays. He has worked on the design and development of infrared, millimeter wave sensors, focal arrays and camera systems.